Experimental modeling of the interaction between waves and submerged flexible mound breakwaters

Elham Jafarzadeh[1], Abdorreza Kabiri-Samani[1] ⑩, Shahriar Mansourzadeh[2] and Asghar Bohluly[3]

Abstract

A submerged flexible mound breakwater can be employed for wave control in shallow water as an advanced alternative to the conventional rigid submerged designs. This study presents a flexible breakwater with an innovative geometry based on model experimentation. Experimental studies were performed to compare the wave energy dissipation by the flexible mound and rigid structures, over a range of test conditions, for example, three different diameters of structure, three water depths, and different regular wave heights for three different beach slopes. Results indicate that the present submerged flexible mound breakwater is stable, being appropriate for most operational sea conditions. Large amplitude waves can induce significant motions of the structure; therefore, the interaction between radiating and scattering waves is highly contributing to the wave energy dissipation. The wave energy dissipation at breaking zone of the present submerged flexible mound breakwater is significantly greater than that of the other types of flexible and rigid formerly investigated structures.

Introduction

One of the major objectives of the coastal and port engineering works is to assure coastline stability. Being exposed to waves, tides, wind, and human activities, the coastline is subjected to change and destruction. Hurricanes at coastlines cause destruction to the nearby coastal structures. The fierce storms rip apart sand dunes and increase the sea level drowning the beaches, changing the coastline profile, thereby causes instability of the coastline, threat the installations and losses investments. Natural dunes are formed when the wind blows the sand across the beach, causing a sand build-up.[1] Unnatural dunes are formed by human at the back of the beach, disrupting the natural tendencies of the beach, thereby promote the beach erosion and thus destroy the native organisms' habitats. Furthermore, they are destroyed in storms more easily than natural dunes and are expensive to maintain and rebuild.[2] Due to the different wave loads and boundary conditions, prevailing on the slope and the crest of a coastal structure, different stability conditions and stability equations have been developed in the literature.[3–6]

Considering economic constraints, low-level submerged coastal structures are generally more stable with a lower cost.[7] An appropriate design of the submerged breakwaters may cause beach restoration by trapping the natural sediments, having lower construction cost compared to the other types of detached breakwaters. These advantages of submerged breakwaters over conventional structures make them more feasible for protecting natural and developed beaches.[8]

[1]Department of Civil Engineering, Isfahan University of Technology, Isfahan, Iran
[2]Subsea R&D Center, Isfahan University of Technology, Isfahan, Iran
[3]Institute of Geophysics, University of Tehran, Tehran, Iran

Corresponding author:
Abdorreza Kabiri-Samani, Department of Civil Engineering, Isfahan University of Technology, P.O. Box 84156, Isfahan, Iran.
Email: akabiri@cc.iut.ac.ir

The submerged breakwaters are effective coastal protection features for recreational and residential coastal areas due to their reduced environmental and visual unfavorable impacts. Due to the submergence, they are less vulnerable to wave action, consequently, are not encouraged to severe wave breaking. The studies performed on solid and permeable submerged breakwaters indicate that these breakwaters with near zero submergences are capable of reducing the incident wave energy by about 50%.[9] Raman et al.[10] assessed the damping action of rectangular and rigid vertical submerged barriers and expressed the transmission coefficient C_t, in terms of the transmitted energy to the total energy of the incident wave. A submerged breakwater with a crest at or below the still water level causes substantial wave attenuation, being highly effective coastal structure. Wave energy damping or wave height attenuation through submerged breakwaters is the major aspects of these structures.[11–16]

Submerged sand/gravel-filled geotextile bags (geobags) are semi-rigid structures, implemented in a few weeks, with relatively low installation cost, have become increasingly popular as an alternative to conventional rigid structures, especially when rapid implementation of stabilization measures are required.[17] There are several investigations to improve the submerged geo-bags performance.[18–22] Comprehensive reviews on the applications of geo-synthetics and geo-containers in hydraulic engineering and for protection of land-fills and coastal areas, which provide valuable information and inspiration for the application of these structures in coastal engineering, have been implemented.[23–28]

The submerged breakwaters usually require vast cross-sectional areas, having significantly increased construction cost along with unfavorable effects on the environment of the covered area. To overcome these criticisms, a thin membrane bag filled with water, namely, "flexible mound" breakwater was first proposed by Tanaka et al.[29] Even for deep submergences, a membrane bag can still reduce wave height significantly, whereas, a corresponding rigid type with the same configuration can hardly affect the transmitted wave height.[29] Kiyokawa et al.[30] applied a simplified one-freedom system, namely, "radiation wave generator," consisting of a movable flat plate connected to a spring-damper system to investigate the mechanisms of wave energy dissipation around the flexible mound breakwaters. Ohyama et al.[31] performed a numerical analysis based on the linear potential flow theory, modeling the membrane as a lumped-mass system, to examine the transmission and reflection characteristics of waves over the flexible mound breakwaters, validated by the experimental data. They declared that motion of the flexible mound breakwater against the incident waves, generates radiation waves, interacting with both the incident and scattering waves. Due to this interaction at a certain wave frequency, no wave transmission over the flexible mound breakwaters occurs.

Based on a preliminary study on the membrane bags, it is reported that the membrane bags have a motion response against the incoming waves, even though the bag is pressurized to be rigid and fix.[32] The experimental results indicated that the response of a membrane bag reduces the transmitted wave height for a wide range of wave frequency. Tanaka et al.[33] carried out experimental studies to examine characteristics of the wave energy dissipation by the flexible mound breakwaters compared to those by the rigid ones. They identified the appropriate ranges of important parameters, affecting the efficiency of flexible type breakwaters. Numerical studies were also performed to assess the mechanism of wave absorption by the flexible structures, indicating that: (1) wave interaction, (2) wave breaking over the structure, and (3) energy loss next to breaking waves are the major issues to influence mechanism of wave dissipation. The interaction of the scattering waves and the radiation waves generated by the membrane motion are highly contributive in wave energy dissipation. The effectiveness of this wave interaction increases, when the scattering and the radiation waves have the same height with an inverse phase. Further to this interaction, the wave breaking significantly increases dissipation of the wave energy, when the crown depth to incident wave height ratio R/H_i is sufficiently small.[33] An example of installing these tubes as a coastal structure was presented in Alvarez et al.,[34] describing the technical solution adopted for the use of geotextile tubes as a semi-covered structure within 4 km of the Yucatan coastline, Mexico. Bloxom et al.[35] experimentally investigated three different incident wave angles and water depths for several wave heights corresponding to different sea states, where the structure angle was 45° to the incident waves' direction, leading to generation of highly nonlinear wave conditions, and thus, wave over-topping and oscillatory motions of the structure. Inflatable membranes filled with water were numerically investigated by Yim,[36] to simulate the dynamics of a mobile platform, subjected to the wave action.

In this study, an innovative design of the submerged flexible mound breakwaters is proposed based on model experimentation. As the wave energy dissipation by a submerged flexible mound breakwater is greater than that of a rigid submerged structure, greater wave energy dissipation is expected due to highly deformed shape of the structure. A comprehensive experimental study is carried out to investigate the influence of flexible mound breakwaters filled with water on the reflection and transmission characteristics of sea waves. Results of this experimental study are compared with those of former flexible and rigid breakwaters in respect to the transmission and reflection coefficients.

Motivation and objectives of this study

Further to the fact that, the construction cost of the submerged flexible mound breakwaters is less than that

of the conventional submerged breakwaters, ships and marine organisms can pass them, if being deep enough. These marine structures reduce the collided wave energy and prevent the generation of standing waves. In the chronology of this science field, different materials can be applied to serve this purpose. The selected design consists of geosynthetic products made of polyethylene and polypropylene materials, which are environmental friendly and can be applied upon the need. Their polymerized feature is cost-effective with high resistance and durability. Moreover in their production process, low greenhouse gases are emitted. These materials do not pollute the environment and can be converted into another source of energy after their lifetime ends. The tubes applied here can resist by earth movement and tolerate flexural and tensile stresses through lightweight. This feature greatly reduces the maintenance cost and its trenching and bedding cost is lower than that of the rigid built up structures. Other advantages of these tubes are their low manufacturing cost, rapid transportation, and low installation time.

Due to importance of the coastal protection in respect to performance, cost, and maintenance, installation of newly designed measures as protective structures is essential. The studies performed on the interaction of waves and determination of the effect of membrane motion against incident sea waves are rare, focusing mostly on the motion of such structures related to the connection to their base as a one-freedom system. The present submerged flexible mound breakwater consists of a multi freedom system, considering type of the tube connection to the base, allowing the structure to move as a spring-damper system. The prevailing constraint of the former studies is the proper performance of the system at certain frequencies. In this study, these limitations are removed; thereby, the system can perform at several frequencies, leading to greater wave energy losses. In general, this study aims to determine the amount of wave energy dissipation, reflection, and transmission based on the model experimentation.

Dimensional analysis

The first step in simulating and modeling is the identification of the variables affecting the physical phenomenon. Adapting a method capable of producing a combination of effective parameters in respect to the physical definition is essential to reduce the number of variables. The governing variables of flow, wave, and structural features are as follows:

- Flow and wave hydraulic characteristics: water depth at the footprint of the structure h, incident wave height H_i, breaking wave height H_b, incident wave length L, and gravitational acceleration g.
- Structural properties: tube equivalent diameter D and slope of the beach S.

Therefore, the energy features of a flexible structure depend on the following parameters

$$H_t, H_r = \text{f}(D, h, H_i, H_b, L, S, g) = 0 \qquad (1)$$

where f is the functional symbol, H_t is the transmitted wave height, and H_r is the reflected wave height. Applying the dimensional analysis of Buckinghum π-theorem, equation (1) is simplified as

$$\text{f}\left(\frac{H_t}{H_i}, \frac{H_r}{H_i}, S, \frac{h}{D}, \frac{S}{\sqrt{\frac{H_b}{L}}}, \frac{H_i}{L}\right) = 0 \qquad (2)$$

The Iribarren number $\xi = S/(H_b/L)^{0.5}$ is a dimensionless parameter applied to recognize different issues of breaking surface gravity waves at the beaches and close to the coastal structures.[37] Accordingly, the dimensionless reflection and transmission coefficients $C_r = H_r/H_i$ and $C_t = H_t/H_i$, respectively, are expressed as

$$C_r, C_t = \text{f}\left(S, \frac{h}{D}, \xi, \frac{H_i}{L}\right) \qquad (3)$$

By evaluating the present test results, the effects of different relevant parameters affecting C_r and C_t are examined.

Experiment setup and apparatus

Schematic of the submerged flexible mound breakwaters and the related parameters studied in this study are shown in Figure 1. The experiments were carried out in a towing tank 108 m long, 3 m wide, and 2.5 m deep at the Hydrodynamic Laboratory of Sub-sea Research and Development Center, Isfahan University of Technology, Iran. A plunger-type wave maker, having a triangular section is applied to generate regular waves with different frequencies, traveling along the towing tank. The specifications of the generated waves are shown in Table 1. The wave frequencies were controlled by the speed of a rotor through a potentiometer, thereby the amplitude of the plunger was adjusted.

Measurements of the free-surface elevation were made by parallel wires of 1.5 mm in diameter and a gap of 6.5 mm, resistance gauges at seven different locations (Figure 1). The wave characteristics in the flume were determined by measuring water level oscillations. The still water depth was constant ($d = 2.2$ m, Figure 1). The essential points in this setup are as follows:

1. The first gauge was placed at the toe of the sloped bottom, 82.8 m far from the wave maker.
2. The distance between the fifth gauge and the horizontal bottom was 0.9 m.
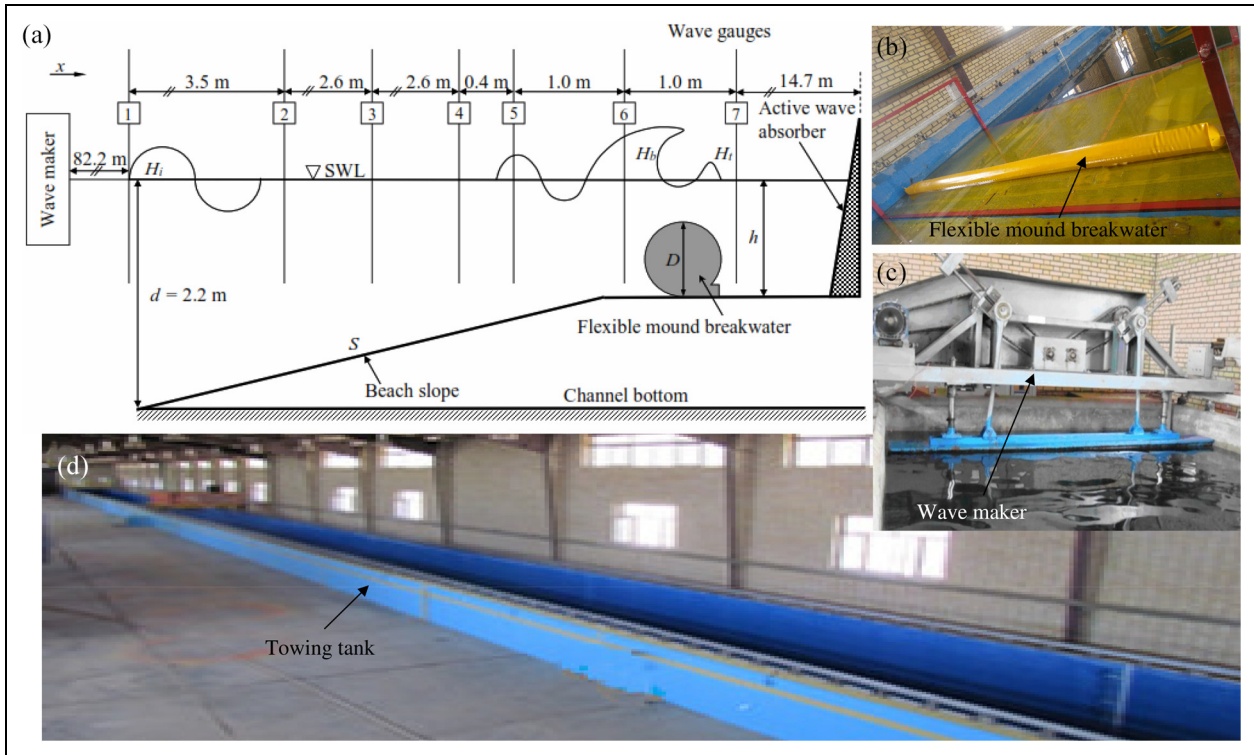3. Seventh gauge was located at a distance of 11.1 m from toe of the sloped bottom.

Figure 1. The experimental setup (a) schematic of the experimental setup and test apparatus, (b) a flexible mound breakwater, installed over the beach, (c) wave maker, and (d) towing tank.

Table 1. Specification of plunger-type wave maker.

Plunger frequency	Motor power (kW)	Plunger length (mm)	Plunger width (mm)	Plunger height (mm)	Plunger amplitude (mm)
Variable	5.5	3000	330	430	150

The wave gauges were calibrated just before each run. The signals generated by the gauges were recorded by a data acquisition system linked to a personal computer. The reflection and transmission coefficients were analyzed for both cases of with and without the submerged flexible mound breakwaters. Significant wave heights and other characteristics are shown in Table 2. The primary tests were performed with two beach slopes of 0.09 and 0.14 without the flexible mound breakwater followed by the tests with the submerged flexible mound structures, installed over the horizontal bottom, about 93 m from the wave generator (Figure 1). The flexible mound breakwaters were made of reinforced rubber membrane fiber with a Young's modulus of elasticity $E = 5800 \, \text{N/cm}^2$, density of $\rho_s = 1.2 \, \text{g/cm}^2$, and thickness of $\varepsilon = 1.5 \, \text{mm}$. The models were sealed to be water tightness hermetically and filled with water. A rigid submerged model was examined to investigate the effectiveness of the submerged flexible mound breakwaters movability on wave dissipation. The model configuration and the wave conditions are shown in Tables 2 and 3. Overall, 16,384 data were

recorded by each gauge with a sampling frequency of 200 Hz.

Time-dependent wave height records

During the first 15 s (for $T = 1.16$ s), the wave traveling from the wave generator toward the first gauge becomes stable at $t = 15$–60 s, applied for estimating the energy spectral, using the wave heights, recorded by the sixth gauge with a submerged flexible mound breakwater (Figure 2).

For $t = 0$–30 s (for $T = 1.16$ s), the waves established by the wave generator cross over the structure, until they reach the seventh wave gauge, where some disturbances appear in the shape of the transmitted waves for a few seconds, followed by the wave stability for $t = 38$–43 s, allowing determination of the transmitted and reflected wave height. Consequently, the wave energy is damped by a wave absorber. Comparing the energy spectrum for the cases with and without the submerged flexible mound breakwater, it is evidence that

Table 2. Dimensional and dimensionless hydraulic aspects of the tests in this study.

Test #	h (m)	H (m)	S	D (m)	D/h	H/L	Test #	h (m)	H (m)	S	D (m)	D/h	H/L
E1–E5	0.36	A[a]	0.09	0.21	0.58	B[b]	E106–E110	0.27	A	0.17	0.14	0.52	B
E6–E10	0.36	A	0.09	0.14	0.39	B	E111–E115	0.27	A	0.17	0.1	0.37	B
E11–E15	0.36	A	0.09	0.1	0.28	B	E116–E120	0.27	A	0.17	0.1-R	0.37	B
E16–E20	0.36	A	0.09	0.1-R[c]	0.28	B	E121–E125	0.23	A	0.09	0.21	0.91	B
E21–E25	0.36	A	0.14	0.21	0.58	B	E126–E130	0.23	A	0.09	0.14	0.61	B
E26–E30	0.36	A	0.14	0.14	0.39	B	E131–E135	0.23	A	0.09	0.1	0.43	B
E31–E35	0.36	A	0.14	0.1	0.28	B	E136–E140	0.23	A	0.09	0.1-R	0.43	B
E36–E40	0.36	A	0.14	0.1-R	0.28	B	E141–E145	0.23	A	0.14	0.21	0.91	B
E41–E45	0.36	A	0.17	0.21	0.58	B	E146–E150	0.23	A	0.14	0.14	0.61	B
E46–E50	0.36	A	0.17	0.14	0.39	B	E151–E155	0.23	A	0.14	0.1	0.43	B
E51–E55	0.36	A	0.17	0.1	0.28	B	E156–E160	0.23	A	0.14	0.1-R	0.43	B
E56–E60	0.36	A	0.17	0.1-R	0.28	B	E161–E165	0.23	A	0.17	0.21	0.91	B
E61–E65	0.27	A	0.09	0.21	0.78	B	E166–E170	0.23	A	0.17	0.14	0.61	B
E66–E70	0.27	A	0.09	0.14	0.52	B	E171–E175	0.23	A	0.17	0.1	0.43	B
E71–E75	0.27	A	0.09	0.1	0.37	B	E176–E180	0.23	A	0.17	0.1-R	0.43	B
E76–E80	0.27	A	0.09	0.1-R	0.37	B	E181	0.36	0.059	0.17	WFMB[d]	–	0.017
E81–E85	0.27	A	0.14	0.21	0.78	B	E182	0.36	0.082	0.17	WFMB	–	0.028
E86–E90	0.27	A	0.14	0.14	0.52	B	E183	0.36	0.097	0.17	WFMB	–	0.039
E91–E95	0.27	A	0.14	0.1	0.37	B	E184	0.36	0.059	0.14	WFMB	–	0.017
E96–E100	0.27	A	0.14	0.1-R	0.37	B	E185	0.36	0.082	0.14	WFMB	–	0.028
E101–E105	0.27	A	0.17	0.21	0.78	B	E186	0.36	0.097	0.14	WFMB	–	0.039

[a]A = 0.059, 0.082, 0.097, 0.107, and 0.123 m.
[b]B = 0.017, 0.028, 0.039, 0.051, and 0.068.
[c]R denotes the tests with a submerged rigid breakwater.
[d]WFMB denotes the tests without a submerged flexible mound breakwater.

Table 3. Characteristics of the generated waves.

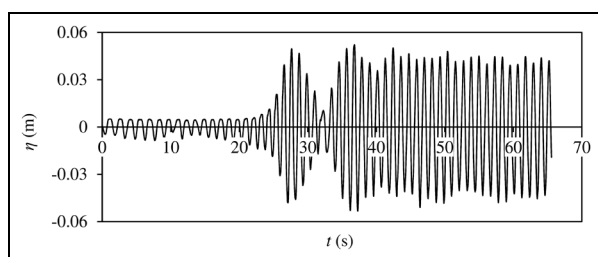| Plunger frequency (Hz)	Wave period (s)	Wave frequency (Hz)	Wave length (m)	Wave height (mm)
0.66	1.5	0.66	3.55	59
0.73	1.36	0.73	2.9	82
0.79	1.26	0.79	2.5	97
0.85	1.16	0.86	2.1	107
0.92	1.06	0.94	1.8	123

Figure 2. Time-dependent water free surface η, for $H = 0.107$ m and $T = 1.16$ s, recorded by the sixth gauge with a submerged flexible mound breakwater.
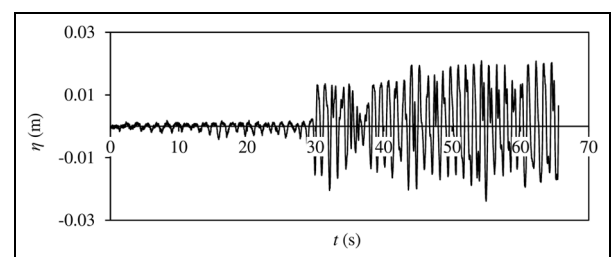

Figure 3. Time-dependent water free surface η, for $H = 0.107$ m and $T = 1.16$ s, recorded by the seventh gauge with a submerged flexible mound breakwater.

the changes in water level at $t = 32$ s (Figure 2) and at $t = 37$ s (Figure 3) are due to the effects of the structure.

Observations

According to the observations of this study, due to deformation of the applied flexible breakwaters for low amplitude waves $H_i/L = 0.017$–0.039, the interference of the scattering and radiation waves did not occur, having no particular effect on the wave height. The breaking waves were observed for these ratios, before reaching the structure. For $H_i/L = 0.05$–0.068, due to the interaction of the radiation waves and the structure, a foamy region looking like a broken wave condition was observed. The location of the breaking wave zone
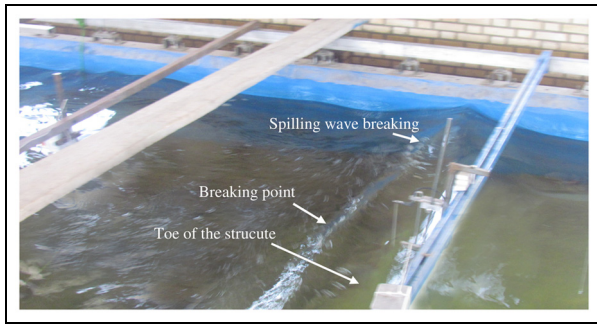
Figure 4. Spilling wave breaking around a submerged flexible mound breakwater, for $S = 0.17$, $D = 0.1$ m, and $h = 0.27$ m.

Figure 6. Broken wave around a submerged flexible mound breakwater due to the low submergence depth, for $S = 0.17$, $D = 0.14$ m, and $h = 0.27$ m.

Figure 5. Wave pattern around and over a rigid breakwater, for $S = 0.17$, $D = 0.1$-R, and $h = 0.27$ m.

Figure 7. Photograph of the wave on a submerged flexible mound breakwater for $S = 0.17$, $D = 0.21$ m, and $h = 0.27$ m.

or the interaction of the reflection and radiation waves is affected by the submergence depth of the flexible structure, moving farther from the structure. Formation of a spilling wave break due to the wedge motion is shown in Figure 4. Spilling wave break might be initiated by a small curl at the wave crest,[38] in which the jet impact with the wave face generates a small region of turbulence close to the flexible structure. This mechanism continues by an instability, forming a swell at the front face of a steep gravity wave.[39]

The location of the breaking zone or collision of the two reflection and radiation waves became farther from the structure, while the submergence depth was significantly increased. Compare these observations with those of a rigid structure, that turbulent region and/or surface air bubbles were not seen around the structure (Figure 5). It was deduced that motion of the inflatable structures significantly affects the wave energy dissipation. At lower submergence depths, a bubbling free surface surrounded by small air bubbles was observed near the structure. According to Figure 6, for an inflatable structure with a beach slope of 0.17, a diameter of 0.14 m, and a submergence depth of 0.13 m, due to low submergence depth, the wave break and collision zone were moved closer to the structure, having the least remained energy.

The structural displacement includes a rotational motion of the structure relevant to its axis. The displacement angle varies, subject to the test conditions, indicating a direct relation between this angle, the wave
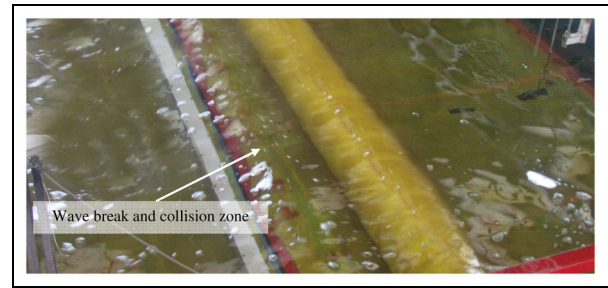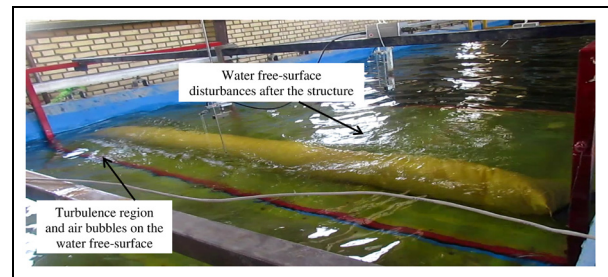
pattern, and free-surface turbulence (Figure 7). We noted that, decreasing the structure diameter, limits the bubbly flow movement upward. Figure 7 also shows that for the maximum beach slope, disturbances were launched before and over the structure.

Increasing the flexible mound structure diameter or decreasing the submergence depth results in the decrease of the transmitted wave height and turbulence intensity thereafter. This is partly due to the positive effect of the obstacle height against the incident wave. These results are consistent with those of Heikal et al.[40] and Yuliastuti and Hashim,[41] who reported that the transmission coefficient C_t decreases as the breakwater height increases. When the breakwater crest is at the water free-surface level, the transmission coefficient is 0.7, independent on the wave steepness. While $H_i/L \geqslant 0.05$, the structural deformation increases, thereby the turbulence intensity and energy dissipation raise, even though the transmitted wave energy is increased too.

According to El-Fiky et al.,[42] Cokgor and Kapdasli,[43] and Shirlal and Rao,[44] transmission coefficient decreases as the wave steepness increases and for $H_i/L \geqslant 0.05$, waves are broken completely over the structure. Observations confirm that the waves are suffered to an intensified turbulence in the vicinity of the structure as the beach slope increases. At lower water depths, waves reach the water breaking point faster; therefore, higher slopes provide more favorable conditions. By examining submerged flexible mound
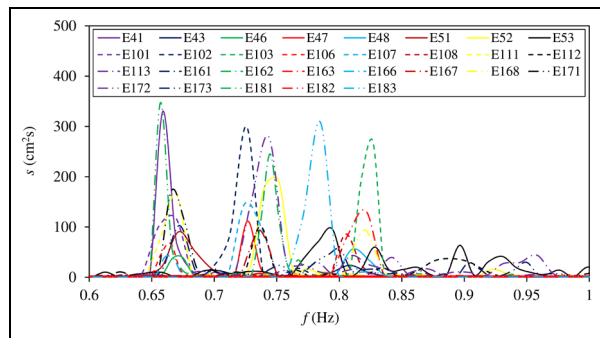
Figure 8. Spectral densities of the cases without and with the submerged flexible mound breakwater for all the water depths at $S = 0.17$ and $H_i = 0.059$, 0.082, and 0.097 m.

Figure 9. Spectral densities of the wave energy for different beach slopes and hydraulic conditions for $H_i = 0.097$ m.

breakwaters with different beach slopes, Seabrook and Hall[45] revealed that an increase in slope tends to increase the wave transmission coefficient. Considering a rigid and a flexible mound breakwater with the same diameter and submergence depth, more turbulence intensity and greater energy dissipation belong to the flexible one, attributed to the structural deformation and wave collision. Stamos et al.[46] experimentally assessed the submerged rectangular and semi-cylindrical rigid and flexible breakwaters, indicating that the rectangular rigid and flexible breakwaters are more effective than the semi-cylindrical breakwaters. They also reported that wave transmission from flexible rectangular model is 14% smaller than that of the corresponding semi-cylindrical model.

Test results and discussion

Wave energy

Applying the measured data, we investigated the effects of flexible mound breakwaters on wave energy by performing a spectral analysis in the MATLAB software, exploring the impact of a submerged flexible mound breakwater. Figure 8 shows the spectral densities for cases with and without a submerged flexible mound structure, obtained by the seventh wave gauge, located after the structure. Comparing the spectral results of different wave attacks showed that the wave energy volume, that is, the sub-spectral area, was higher in the first case (without a structure) than in the second (with a structure). Although the spectral density decreased after the breaking phenomenon located on the submerged breakwater, no significant changes were observed, propagating toward the beach. Figure 8 shows the measured data by a gauge installed next to the structure for different water depths, diameters of the structure, wave heights and a beach slope of 0.17, with the maximum generated wave energy being associated with the case without the submerged flexible mound breakwater. The maximum wave energy at a 0.097-m height of the incident wave decreased from 52.36 to 46.05 J after breaking over the submerged breakwater.
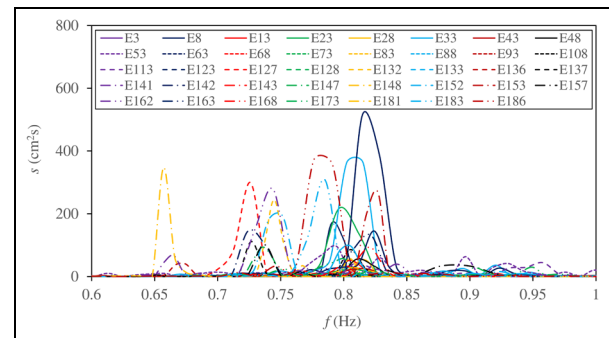
Figure 8 shows that a submerged flexible mound breakwater acts as a wave generator in shallow water by taking advantage of the structure displacement, and that the collision of the radiated and reflected waves around the structure further decreases the wave energy. According to Figure 8, frequency changes by the structure movements, increased with increase in the wave energy. Moreover, comparison of the extracted spectra for different diameters of the structure and submergence depths showed that the maximum energy after the structure was generated with the minimum diameter and the lowest submergence depth. The same held true for the largest diameter and highest submergence depth. The structure movements were inadequate at the minimum diameter, and the wave passed over the structure more easily while interacting less with the structure at the maximum diameter and deepest submergence depth. For the minimum and maximum structure diameters, the maximum energy was obtained at an average diameter of 0.14 m, which allowed for a better attenuation of the wave energy. These findings suggest that the tube movements significantly contributed to reducing the wave energy. At an average diameter, the wave energy decreased with an increase in the submergence depth, suggesting the need for an adequate submergence depth. With the average diameter of the tube and the highest submergence depth, the average reduction in the wave energy was higher at a higher compared to lower wave steepness. This reduction was approximately 92% for a wave steepness of 0.017, 82% for a wave steepness of 0.028, and 73% for a wave steepness of 0.039, suggesting that the tube movement is more effective than high waves at low waves.

The movements of the inflatable structure acting as a wave generator and the interaction between incident wave and the scattering wave dissipated the wave energy. Figure 9 compares the spectral of wave energy, obtained by the seventh wave gauge located after the structure, by examining the effect of beach slopes before the submerged flexible mound breakwater. This

figure shows the variations in the energy spectral for a 0.097-m wave height at different slopes, suggesting a significant decrease in the maximum energy of the incident waves associated with the submerged flexible mound breakwater. The maximum reduction in the wave energy was observed for the maximum value of S at the same wave height. Wave transmission through shoaling occurred as waves perpendicularly approached shallower water where the wave speed and length decreased. Given that the energy flux is conserved, the energy per unit area of the wave changed, and the wave height increased and its period remained constant in shallow water. A decrease in the wave length and an increase in its height or the increase in the wave steepness caused wave breaking.[47–49] The waves approaching shallow water break at relatively middle point of the steeper slope before they reach the structure. Figure 9 shows a decrease in the wave energy with an increase in the beach slope. The wave breaks over the structure for $D/h = 0.27$, that is, a submerged flexible mound breakwater with a diameter of 0.1 m, and the maximum beach slope, reduced the incident wave energy from 32 to 0.6 J.

Wave height

The zero-crossing wave height H was defined as the vertical distance between the highest and the lowest values of the wave recorded with the gauges between two zero-down crossings (or up crossings). This parameter was found to be an appropriate feature for explaining all variations in wave when approaching the structure.[50] Applying H along the flume caused the potential period to appear constant along the flume, while the wave height increased with a decrease in water depth as a result of shoaling and breaking phenomena. Figure 10 shows the water level for $H_i = 0.107$ m at different conditions. In this figure, the results of the same tests repeated with a submerged flexible mound breakwater located at the beach for different diameters of the structure. This figure also evaluates wave heights in some of the tests for all the gauges, suggesting a significant increase in the wave height in front of the structure for the same conditions and an increase in the magnitude and a break in the higher waves in the vicinity of the structure. Given the wave heights and water depths, no wave breaking was possible without the structure in all the experiments even at the maximum beach slope. Therefore, the present structure was appropriate for providing conditions of wave breaking, and it was effective in reducing the wave energy. Figure 10 suggests an initial decrease in incident wave height in the sloped beach followed by a significant increase throughout the section close to the structure as a result of shoaling. Some oscillations were also observed in the wave height. The wave breaking effect therefore significantly reduced the wave height.

Figure 11 shows the wave heights for the incident waves generated with $H_i = 0.107$ m with the break zone
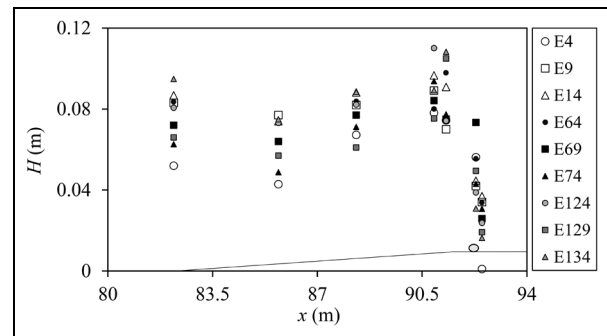

Figure 10. Wave heights for all gauges recorded during different test conditions for all the water depths at $S = 0.09$ and $H_i = 0.107$ m.
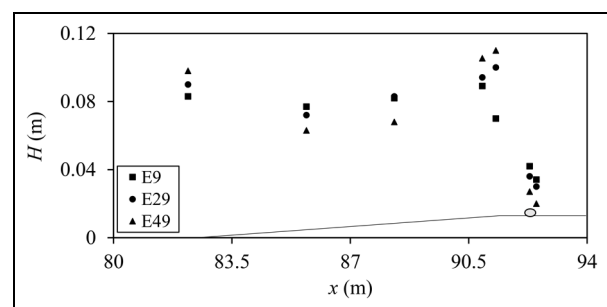

Figure 11. Wave heights for all gauges, changing the beach slope for $D = 0.14$ m and $H_i = 0.107$ m.

varying for different beach slopes and diameters owing to the structural motion. A decrease in the submergence depth at the same beach slope moves the wave break to a location far from the structure. Figure 11 also shows the locations of the wave break at different slopes with the structure lying 92.5 m away from the wave maker. According to this figure, a slope decrease moved the wave break zone away from the structure, making the wave to move more energetically toward the structure. The adequate performance of the maximum beach slope at a low water depth generated a wave break zone close to the structure. To obtain an ideal situation, the potentially significant relationship between the beach slope and submergence depth should be confirmed.

Reflection coefficient

Figure 12 shows variations in H_r of all water depths on the foot of the structure for different submergence depths and structure diameters in different experiments. At a low submergence depth, H_r mainly lay between 0.06 and 0.1, suggesting more reflection compared to that of the other tests. According to this figure, H_i tends to a mild increase in H_r as the wave height is increased, whereas H_i caused no significant changes in H_r for small amplitude waves. The effect of the submergence
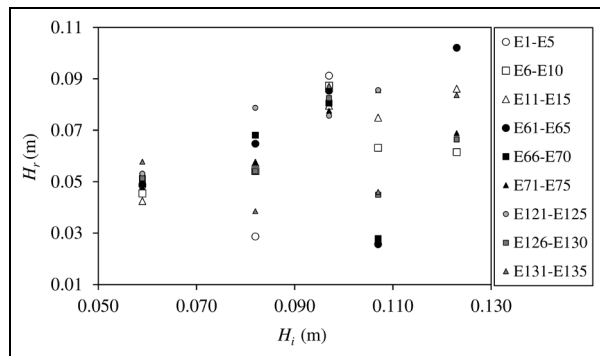
Figure 12. Reflection wave height against incident wave height for all the hydraulic conditions at $S = 0.09$.
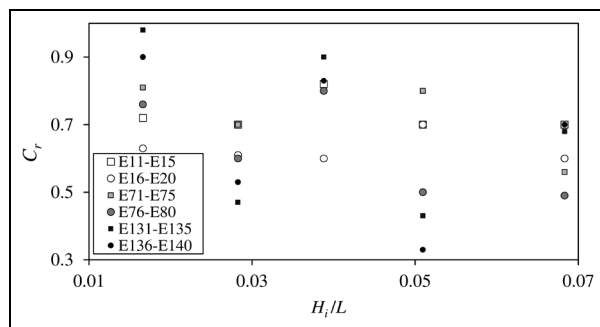

Figure 13. Reflection coefficient of the submerged flexible mound breakwaters compared to that of a rigid structure for all the hydraulic conditions at $S = 0.09$ and $D = 0.1$ m.

depth on H_r of high waves was therefore less evident. This study used the calculation method proposed by Goda and Suzuki,[51] which resulted in a reflection coefficient, outperforming that calculated by Isaacson.[52] Over the sloping beds, the Goda and Suzuki's method has been applied by several investigators.[53–57] Most of them utilized different simplifications to consider wave shoaling and phase shift effects. The water depths studied herein included the deep to medium water depth conditions, thereby this method applies on our measurements. Furthermore, for a better comparison, consistent with Tanaka et al.,[33] the fourth and fifth gauges were used to calculate the reflection coefficient. Comparing a flexible structure with a rigid structure constituted an important part of the present research. Figure 13 shows the changes in the reflection coefficients of the rigid and flexible structures. The cross-sectional connection of the studied structure to a point on the ground resulted in its circular shape and caused the movements of the submerged flexible mound breakwater to yield more effective results compared to those obtained from the other designs.

Flexural movements significantly affect the wave reflection. The two reflection coefficients approached each other at high altitudes given the low diameter effect. Therefore, the effect of submergence is minimal at lower wave heights. The structure movement was

highly effective in the reflection coefficient even at low wave heights. The reflection coefficient of a rigid structure was below that of a flexible structure. A submerged flexible mound structure was different from a rigid one by approximately 30% at a 0.23-m water depth. The negligible difference between a rigid and a flexible structure at a wave height of 0.059 m increased with the wave height. At a 0.082-m wave height, a reflection coefficient of 0.04 was obtained, suggesting that a rigid structure transmits lots of the wave energy. The reflection coefficients of the flexible and rigid structures were the same at a 0.36-m water depth, demonstrating the improved performance of the rigid structure, by increasing the submergence depth.

Figure 14 compares the present findings with those obtained from numerical solutions and experimental data of Tanaka et al.[33] as a function of H_i/L, where solid points represent the possible breaking conditions for 0.107–0.123 m incident wave heights. Given the relatively higher possibility of wave breaking at these points, their distance was high from the points found by Tanaka et al.,[33] who examined this structure when bottom connected at two sides to the ground, which only allowed for movements on the surface. The reflection coefficient was 0.8–1 at the low submergence depths. An increase in the submergence depth significantly reduced its effect on the reflection coefficient, which was expected as the likelihood of wave breaking decreased with an increase in the submergence depth. The reflection coefficient was minimized at maximum values of H_i in all the conditions, which can be explained by the fact that an increase in the wave height suddenly changed the velocity and acceleration of water particles, caused turbulence and wave energy dissipation and ultimately led to wave breaking or interactions between the incident and scattered waves. The reflection coefficient was maximized at a 0.14-m diameter and a 0.27-m water depth. The present findings suggest the necessity of minimizing the submergence depth to increase the reflection coefficient. The reduction in C_r of the present flexible structure was therefore further reduced by 0.1–0.2 with a decrease in the submergence depth. A decrease in wave steepness for different water depths made the reflection coefficients closer to one another, and an increase in wave steepness resulted in C_r values different from one another by approximately 50%.

The effect of changes in water depth can therefore be neglected at a low wave steepness. The C_r reported in some experiments was close to unity, as the scattered and the radiated waves were of the same height and opposite phases.[33] A decrease in the effect of the submergence ratio on C_r together with an increase in wave height was inevitable, suggesting a 0.6–0.7 decrease in the submergence depth ratio. More movements of small structures caused C_r to increase with a decrease in water depth at relatively large amplitude waves. At a maximum wave steepness, maximizing the structure diameter maximized reflection, suggesting a relationship
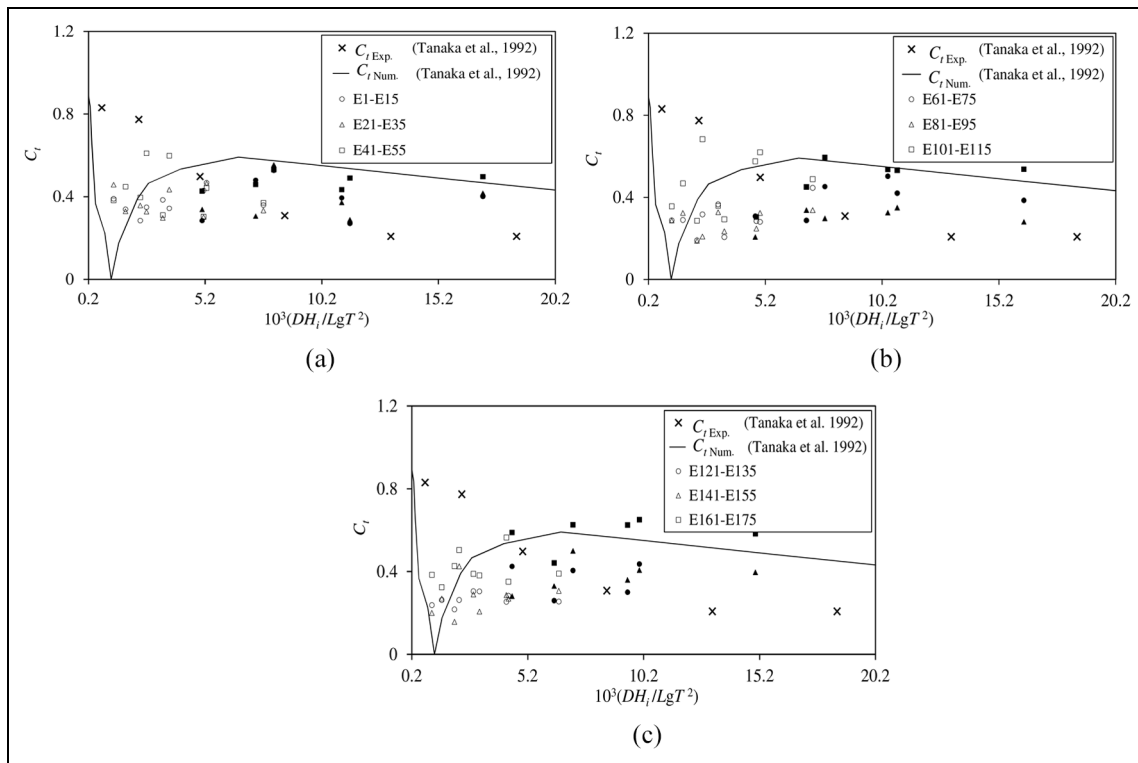
Figure 14. Reflection coefficient versus $10^3(DH_i/LgT^2)$ for (a) $1.6 > h/D > 2.3$, (b) $1.9 > h/D > 2.7$, and (c) $2.6 > h/D > 3.6$.

between diameter and the reflected wave height. At a minimum wave steepness, no significant changes were observed in C_r with changes in diameter. The minimum diameter maximized reflection coefficient at a 0.107-m wave height. Insignificant variations were observed in C_r in terms of H_i/L in all the test models at low wave heights. An increase in the wave height also increased C_r, and a small diameter and low heights were found potentially more effective owing to the more movements of the flexible structure. The smallest diameter was, however, associated with the highest reflection, suggesting that the relationship between the structure diameter and the wave height can be optimized to maximize the reflection coefficient.

According to Figure 14, the present experimental results are well correlated with those of the former experimental and numerical results. Energy dissipation was higher in this study compared to in the former studies owing to more movements of the structure. Wave breaking in the newly proposed flexible mound structure can significantly contribute to dissipating the wave energy. Wave breaking at a 0.107-m wave height decreased C_r, making turbulence in the structure, and C_r was maximized at a 0.123-m wave height compared to in the other tests.

Transmission coefficient

Figure 15 shows the transmission wave height as a function of wave steepness. According to this figure, H_t increased with H_i except at certain points of wave
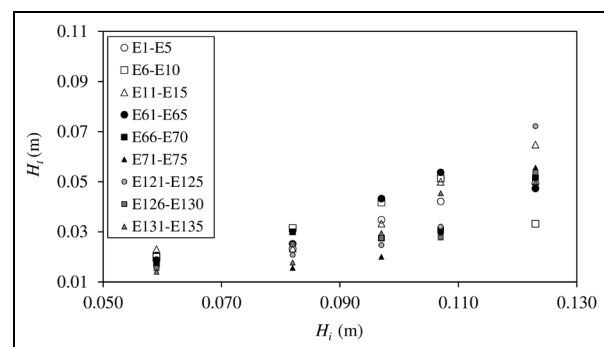

Figure 15. Transmitted wave height versus incident wave height of different test conditions for all the hydraulic conditions at $S = 0.09$.

breaking with a 0.107–0.123-m wave height. Figure 15 shows no differences between the results obtained for different structure diameters at the lowest wave height, suggesting that the coefficients of transmission were close to one another.

At lower transmission coefficients and higher H_i, performance was the same for the minimum structure diameter of 0.10 mm and the maximum diameter of 0.21 mm. At 0.107 and 0.123-m wave heights, wave breaking or confrontation of radiated and reflected waves changed the conditions, and the structure performance was better at a 0.123-m wave height and a 0.14-mm diameter as well as a 0.107-m wave height and a 0.21-mm diameter. Given the greater submergence
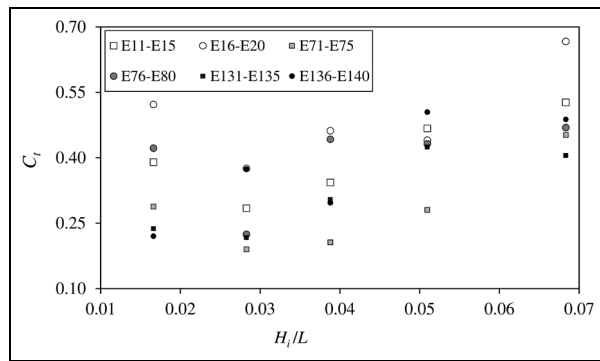
Figure 16. Changes of transmission coefficient for the submerged flexible mound breakwaters compared to those of the rigid structure for all the hydraulic conditions at $S = 0.09$ and $D = 0.1$ m.

depth at a 0.10-m diameter, the transmission coefficient was maximized at a 0.21-m diameter. At a low wave steepness, performance was better at the highest and the lowest submergence depths. In case of breaking or colliding waves with the same submergence depth, the transmission coefficient and wave passage over the structure were decreased.

Performance was similar in all the three structures with different diameters and a low wave steepness and 0.27 and 0.36 m water depths. At a 0.27-m water depth, the smallest diameter was associated with the minimum transmission coefficient with an increase in the wave height, and the largest diameter caused an appropriate performance at only a 0.123-m wave height given the wave breaking on the structure at a large diameter. A similar behavior was observed for different diameters of the structure at a 0.36-m water depth and a small wave steepness. At a 0.107-m wave height, both 0.21 and 0.14 m structure diameters led to similar results, and at a 0.123-m wave height, similar performance was observed for diameters of 0.10 and 0.14 m. The transmission coefficient was therefore found to be minimized at a 0.27-m water depth and a diameter of 0.10 m, which suggests the need for performing further studies to optimize the transmission coefficient based on the submergence depth. For the maximum wave steepness, the higher the water depth, the greater the transmission coefficient reduction was resulted in.

According to Figure 15, the deepest water with a lower H_t performed better at a 0.21-m diameter and a low wave steepness, whereas at the highest wave steepness, water depths of 0.36 and 0.27 m led to similar performances. The transmission coefficient decreased at a 0.10-m diameter and a 0.27-m water depth and increased with depth. The transmission coefficient was minimized at a lower wave steepness and a submergence depth of approximately 0.10 m, which can be explained by the structure frequency and the wave produced by the structure against the incident wave. At a high wave steepness, the submergence depth was higher than the average and exerted no significant effects on

the transmission coefficient. The flexibility and movements of this structure reduced the wave energy transmitted. Figure 16 shows changes in the transmission coefficients of the rigid and flexible structures, with the average value of the flexible structure being lower than that of the rigid structure by 25% at a 0.23-m water depth, by 52% at a 0.27-m water depth, and by 15% at a 0.36-m water depth. The quite similar performance of the structures at some points can be attributed to an increase in the water depth at a higher wave steepness. The results showed that the structure performance was optimized at an average water depth of 0.27 m. Overall, the submerged flexible mound breakwater results in better structural performance in dampening the wave energy compared to a rigid one.

Figure 17 depicts the transmission coefficient as a function of the wave steepness in this study as well as the experimental and numerical data obtained by Tanaka et al.[33] for a tube connected to the bottom at two sides. The results of this study are consistent with the experimental and numerical data obtained by Tanaka et al.[33] The interaction between waves is the main cause of energy loss in submerged flexible mound breakwaters. The solid points corresponding to 0.107 and 0.123 m wave heights have potential for wave breaking.

The transmission coefficients of some points were higher than the reference results with the lowest transmission coefficient, owing to the possibility of turbulence on the water free surface in the breaking zone as recorded with the gauges, which was supported by high reflection coefficients at these points. The transmission coefficient was negligible compared to the reference results and no wave was transmitted from the structure at some points in this diagram, which can be explained by the natural frequency of the flexible structure. At these points, only the vibrations and turbulence of the surface were likely to be recorded with the gauge after the structure, and the close-to-zero values suggested low levels of perturbation after structure.

The effect of different beach slopes was investigated in different conditions by focusing on the wave height approaching the coast and after overpassing the structure at different conditions. The equations governing the wave movement toward the beach show that an increase in the slope precipitated the wave breaking, and a decrease in the wave height over the structure reduced the wave energy. According to Figure 17, the transmission coefficients associated with slopes of 14% and 17% were insignificantly different. The performance associated with a beach slope of 9% resembled that of the other slopes at some of down wave heights such as 0.059 and 0.082 m, which suggested the insignificant effect of slope at low wave heights. The effect of a high beach slope was, however, increased by about 45% compared to that of a mild slope by increasing the wave height and decreasing the water depth and approaching the breaking conditions. Given beach slope as a key factor and that a lower depth provided
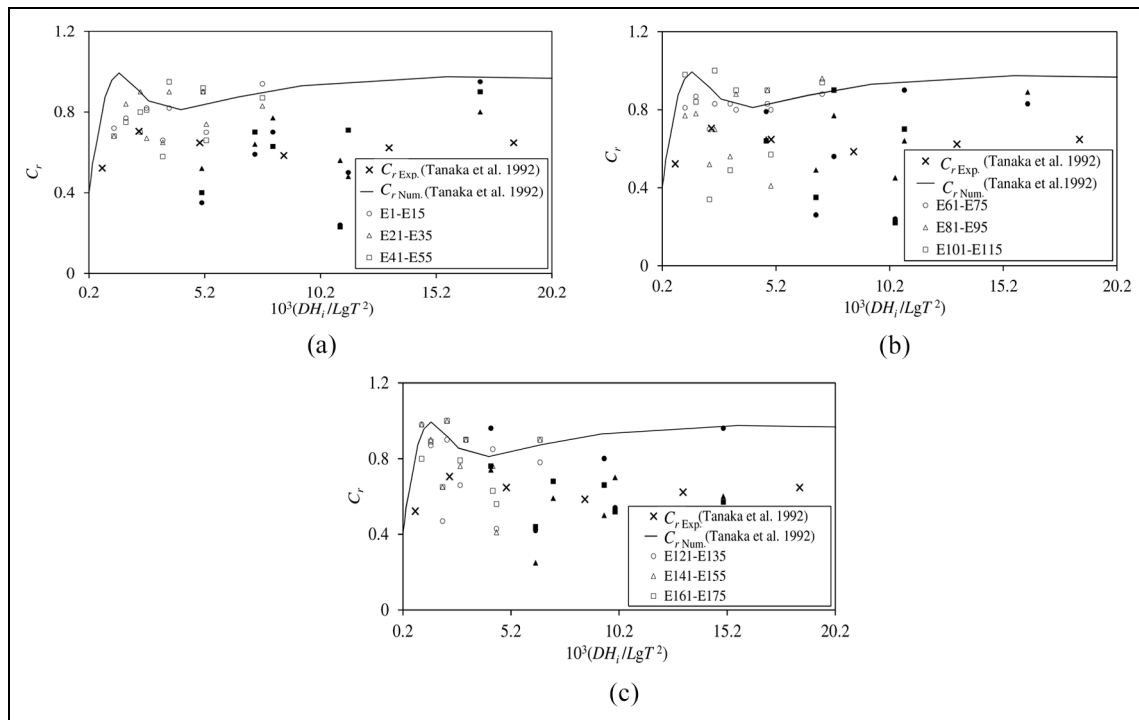
Figure 17. Transmission coefficients obtained in this study compared to those of Tanaka et al.[33] for (a) $1.6 > h/D > 2.3$, (b) $1.9 > h/D > 2.7$, and (c) $2.6 > h/D > 3.6$.

conditions for wave breaking, the difference between the three slopes was about 50% at a 0.23-m water depth and an average of 20% at 0.27 and 0.36-m water depths. According to the present results, wave breaking through flexible mound structures can significantly contribute to dampening the wave energy, thereby reducing the transmission coefficient. Whereas, in similar conditions, a rigid structure cannot reduce the transmitted wave height as the waves are transmitted from the structure without breaking.

Wave breaking type including spilling, plunging, collapsing, or surging is generally related to the Iribarren number ξ, describing the wave behavior at a beach. Several researchers applied ξ to present criteria for the design and stability of breakwaters. To control the possible damage of waves on coastal structures, the type and mechanism of wave breaker is of essential. By examining the wave steepnesses as well as the beach slopes considered herein, and determining the Iribarren numbers for different hydraulic conditions, we observed just two types of wave breaking in the vicinity of the flexible structures, including spilling and plunging breakers. Most of the incident waves for the minimum beach slope ($S = 0.09$) had a surf similarity parameter at a range of spilling wave breaker ($\xi < 0.5$). However, plunging breaker was also observed for greater submergence depths with the beach slopes of 0.14 and 0.17, having ξ between 0.5 and 1.3. Therefore, the newly proposed submerged flexible mound breakwaters not only reduce the transmission coefficient at the beach but also can significantly increase the intensity of breaking wave along the traveling path.

Conclusion

As an alternative to a conventional rigid breakwater, a submerged flexible mound breakwater comprising a thin membrane bag filled with water for wave control was studied and discussed in this study. We investigated the wave energy dissipation, reflection, and transmission from the submerged flexible mound breakwaters with the wave heights of 0.059–0.123 m. Seven probes were applied to obtain instantaneous water levels and assess the reflection and transmission coefficients as a result of interactions between the flexible structure and waves. Results indicated a wave energy dissipation of up to about 80%, as a consequence of the interaction between the incident/scattered waves and the radiated waves, generated by the membrane motion. The present results demonstrated a better structural performance at higher beach slopes as the waves reached shallow water earlier with a high possibility of breaking along their traveling path. The potentially positive relationship between the transmission coefficient and the structure diameter as well as the submergence depth clarify the fact that for a certain wave steepness, diameter of the flexible structure and the submergence depth should be chosen appropriately.

Assessing the reflection and transmission coefficients for different conditions revealed at least a 15% damping of wave energy by the submerged flexible mound breakwaters. Comparing the findings of the present experimental study with those of former researches suggested that greater displacements and rotations of the present structure tend to the increased performance of the wave energy dissipation. The mechanism of wave

dissipation by a submerged flexible mound breakwater was originated from the interaction between the scattered and the radiated waves generated by the membrane motion. The wave interaction was effective, while the scattered and radiated waves were of the same height and an opposite phase, thereby the transmission coefficient may be zero. For the ranges of hydraulic parameters studied herein, for $0.05 \leqslant H_i/L$, a milder slope S, and a lower water depth at the footprint of the structure (or a lower submergence depth), wave breaking, or confrontation of radiated and reflected waves resulted in an improved performance of the submerged flexible mound breakwaters, allowing for a better attenuation of the wave energy. Moreover, comparing the extracted spectra for different submergence depths, the maximum energy transmission belongs to the lowest submergence depth, suggesting that the tube movements significantly reduce the wave energy. Finally, the present flexible mound breakwater, connected to the base at one side, can serve as an appropriate wave energy dissipater owing to its greater motion as an emergency breakwater during a storm.

Data availability statement

Some or all data, models, or code that support the findings of this study are available from the corresponding author upon reasonable request.

Declaration of conflicting interests

The author(s) declared no potential conflicts of interest with respect to the research, authorship, and/or publication of this article.

Funding

ORCID iD

Abdorreza Kabiri-Samani 🔟 https://orcid.org/0000-0002-5984-3892

References

1. Pilkey OH, Rice T and Neal WJ. *How to read a North Carolina Beach: bubble holes, barking sands, and rippled runnels*. Chapel Hill, NC: UNC Press Books, 2004.
2. Pilkey OH and Neal WJ. North Topsail Beach, North Carolina: a model for maximizing coastal hazard vulnerability. In: Kelley JT, Pilkey OH, Andrew J, et al. (eds) *America's most vulnerable coastal communities*, vol. 460. Boulder, CO: Geological Society of America, 2009, pp.73–90.
3. Oumeraci H, Hinz M, Bleck M, et al. *GroBmaBstabliche Untersuchungen zur hydraulischen Stabilitat geotextiler Sandcontainer unter Wellenbelastung*. LIW—TUB Nr. 878. Braunschweig: Leichtweiss-Institut für Wasserbau, 2002 (in German).
4. Recio J and Oumeraci H. Effect of deformations on the hydraulic stability of coastal structures made of geotextile sand containers. *Geotext Geomembranes* 2007; 25(4–5): 278–292.
5. Recio J and Oumeraci H. Process based stability formulae for coastal structures made of geotextile sand containers. *Coast Eng* 2009; 56(5–6): 632–658.
6. Van Steeg P and Vastenburg EW. *Large scale physical model tests on the stability of geotextile tubes*. Deltares report 1200162-000, 2010, https://repository.tudelft.nl/islandora/object/uuid%3Ab500287f-c3e4-4328-973e-24993176b1c2
7. D'Angremond K, Van Der Meer JW and De Jong RJ. Wave transmission at low-crested structures. *Coast Eng* 1997; 21: 2418–2427.
8. Ahmadian AS and Simons RR. Estimation of nearshore wave transmission for submerged breakwaters using a data-driven predictive model. *Neural Comput Appl* 2018; 29(10): 705–719.
9. Dick TM and Brebner A. Solid and permeable submerged structures. In: *Proceedings of the 11th international conference on coastal engineering*, 1968, pp.1141–1158, https://ascelibrary.org/doi/10.1061/9780872620131.072
10. Raman H, Shankar J and Dattatri J. Submerged breakwater. *Cent Board Irrig Power J* 1977; 34: 205–212.
11. Johnson JW, Fuchs RA and Morison JR. The damping action of submerged breakwaters. *EOS Trans Am Geophys Union* 1951; 32(5): 704–718.
12. Dhinakaran G, Sundar V and Sundaravadivelu R. Review of the research on emerged and submerged semi-circular breakwaters. *Proc IMechE, Part M: J Engineering for the Maritime Environment* 2012; 226(4): 397–409.
13. Hom-ma M and Horikawa K. A study on submerged breakwaters. *Coast Eng Japan* 1961; 4(1): 85–102.
14. Dhinakaran G, Sundar V, Sundaravadivelu R, et al. Performance of a perforated submerged semicircular breakwater due to non-breaking waves. *Proc IMechE, Part M: J Engineering for the Maritime Environment* 2012; 226(1): 36–50.
15. Baba M. Computation of wave transmission over a shore protecting submerged breakwater. *Ocean Eng* 1986; 13(3): 227–237.
16. Mani JS, Vijaykumar S and Mahadevan R. Diffraction of waves by submerged breakwater. In: *Proceedings of the 4th Indian national conference on ocean engineering*, Goa, September 1991, pp.403–407. National Institute of Oceanography.
17. Burcharth HF, Zanuttigh B, Andersen TL, et al. Innovative engineering solutions and best practices to mitigate coastal risk. In: Zanuttigh B, Nicholls RJ, Vanderlinden J-P, et al. (eds) *Coastal risk management in a changing climate*. Oxford: Butterworth-Heinemann, 2015, pp.55–170.
18. Heerten G. Geotextiles in coastal engineering—25 years experience. *Geotext Geomembranes* 1984; 1(2): 119–141.
19. Lefaive E. Durability of geotextiles: the French experience. *Geotext Geomembranes* 1988; 7: 553–558.
20. Santvoort GP. *Geotextiles and geomembranes in civil engineering*. Rotterdam: AA Balkema, 1994.

21. Pilarczyk KW. *Geosynthetics & geosystems in hydraulic and coastal engineering*. Rotterdam: AA Balkema, 2000.

22. Greenwood JH and Friday A. How to predict hundred year lifetimes for geosynthetics. In: *Proceedings of the 8th international conference on geosynthetics*, Yokohama, Japan, 18–22 September 2006, pp.1539–1542. Rotterdam: Millpress. S.

23. Fowler J, Bagby RM and Trainer E. Dewatering sewage sludge with geotextile tubes. In: *Proceedings of the 49th Canadian geotechnical conference*, St. John's, NL, Canada, 23–25 September 1996, pp.1–31. Canadian Geotechnical Society.

24. Lenze B, Heerten G, Saathoff F, et al. Geotextile sand containers-Successful solutions against beach erosion at sandy coasts and scour problems under hydrodynamic loads. In: *Proceedings of the 6th international conference, LITTORAL*, Porto, 22–26 September 2002, pp.375–381. Porto: Associação EUROCOAST-Portugal.

25. Heibaum M, Fourie A, Girard H, et al. Hydraulic applications of geosynthetics. In: *Proceedings of the 8th international conference on geosynthetics*, Yokohama, Japan, 18–22 September 2006, pp.79–120. Rotterdam: Millpress. S.

26. Kavazanjian R, Diwon N, Katsumi T, et al. Geosynthetic barriers for environmental protection at landfills. *Proceedings of the 8th international conference on geosynthetics*, Yokohama, Japan, 18–22 September 2006, pp.121–152. Rotterdam: Millpress. S.

27. Lawson CR. Geotextile containment for hydraulic and environmental engineering. *Geosynth Int* 2008; 15(6): 384–427.

28. Saathoff F, Oumeraci H and Restall S. Australian and German experiences on the use of geotextile containers. *Geotext Geomembranes* 2007; 25(4–5): 251–263.

29. Tanaka M, Mitsumata M, Ohyama T, et al. Experimental study on wave control by a flexible submerged dike. In: *Proceedings of 34th Japan conference on coastal engineering*, Tokyo, Japan, September 1987, pp.492–496. JSCE.

30. Kiyokawa TM, Mitsumata Tanaka M and Ohyama T. Wave control by radiation wave generator. In: *Proceedings of 34th Japan conference on coastal engineering*, Tokyo, Japan, September 1987, pp.472–476 (in Japanese). JSCE.

31. Ohyama T, Tanaka M, Kiyokawa T, et al. Wave deformation on a flexible submerged dike. In: *Proceedings of 34th Japan conference on coastal engineering*, Tokyo, Japan, September 1987, pp.497–501. JSCE.

32. Ohyama T, Tanaka M, Kiyokawa T, et al. Transmission and reflection characteristics of waves over a submerged flexible mound. *Coast Eng Japan* 1989; 32(1): 53–68.

33. Tanaka M, Ohyama T, Kiyokawa T, et al. Characteristics of wave dissipation by flexible submerged breakwater and utility of the device. *Coast Eng* 1992; 20(1): 1615–1624.

34. Alvarez IE, Rubio R and Ricalde H. Beach restoration with geotextile tubes as submerged breakwaters in Yucatan, Mexico. *Geotext Geomembranes* 2007; 25(4–5): 233–241.

35. Bloxom A, Medellin A, Vince C, et al. *Modeling & testing of inflatable structures for rapidly deployable port infrastructures*. Bethesda, MD: Naval Surface Warfare Center Carderock Division, 2010.

36. Yim S. *A feasibility study on numerical modeling of large-scale naval fluid-filled structure contact-impact problems.* Bethesda, MD: Naval Surface Warfare Center Carderock Division, 2011.

37. Iribarren CR and Norales C. Protection des ports. In: *Proceedings of XVIIth international navigation congress*, Lisbon, Portugal, 19–22 September 1949, pp.31–80. PIANC.

38. New AL, McIver P and Peregrine DH. Computations of overturning waves. *J Fluid Mech* 1985; 150: 233–251.

39. Duncan JH. Spilling breakers. *Annu Rev Fluid Mech* 2001; 33(1): 519–547.

40. Heikal EM, Ibraheem AA, Owais TM, et al. Damping action of near-shore trapezoidal submerged breakwaters. *Bull Facul Eng Ain Shams Univ* 2002; 37(1): 235–249.

41. Yuliastuti DI and Hashim AM. Wave transmission on submerged rubble mound breakwater using L-blocks. In: *2nd international conference on environmental science and technology (IPCBEE 2011)*, http://www.ipcbee.com/vol6/no1/55-F00108.pdf

42. El-Fiky GS, Kato T and Fujii Y. Vertical crustal movement in Tohoku District, Japan, deduced from dynamic adjustment of levelling and tidal data. *Bull Earthq Res Inst Univ Tokyo* 1996; 71: 47–71.

43. Cokgor S and Kapdasli MS. Performance of submerged breakwaters as environmental friendly coastal structures. In: Zimmermann C, Dean RG, Penchev V, et al. (eds) *Environmentally friendly coastal protection*. Dordrecht: Springer, 2005, pp.211–218.

44. Shirlal KG and Rao S. Ocean wave transmission by submerged reef—a physical model study. *Ocean Eng* 2007; 34: 2093–2099.

45. Seabrook SR and Hall KR. Wave transmission at submerged rubblemound breakwaters. *Coast Eng* 1999; 15: 2000–2013.

46. Stamos DG, Hajj MR and Telionis DP. Performance of hemi-cylindrical and rectangular submerged breakwaters. *Ocean Eng* 2003; 30(6): 813–828.

47. McCowan J. On the solitary wave. *Philos Mag* 1891; 32: 45–58.

48. Miche R. Mouvements ondulatoires de la mer en Profondeur Croissante ou Décroissante. *Ann Ponts Chausses* 1944; 116: 369–406.

49. Munk WH. The solitary wave theory and its application to surf problems. *Ann NY Acad Sci* 1949; 51(3): 376–424.

50. Martin A. *Wave breaking analysis with laboratory tests*. Lisbon: University of Lisbon, 2013.

51. Goda Y and Suzuki Y. Estimation of incident and reflected waves in random wave experiments. *Coast Eng* 1977; 1: 828–845.

52. Isaacson M. Measurement of regular wave reflection. *J Waterway Port Coast Ocean Eng* 1991; 117(6): 553–569.

53. Rathbun JR, Cox DT and Edge BL. Wave runup and reflection on coastal structures in depth-limited conditions. In: *26th international conference on coastal engineering*, Copenhagen, 22–26 June 1998, pp.1053–1067. Reston, VA: ASCE.

54. Chang HK. A three-point method for separating incident and reflected waves over a sloping bed. *China Ocean Eng* 2002; 16(4): 499–512.

55. Chang HK and Hsu TW. A two-point method for estimating wave reflection over a sloping beach. *Ocean Eng* 2003; 30(14): 1833–1847.

56. Wang SK, Hsu TW, Weng WK, et al. A three-point method for estimating wave reflection of obliquely incident waves over a sloping bottom. *Coast Eng* 2008; 55(2): 125–138.

57. Young DM and Testik FY. Wave reflection by submerged vertical and semicircular breakwaters. *Ocean Eng* 2011; 38(10): 1269–1276.

Appendix I

Notation

C_r	reflection coefficient $(-)$
C_t	transmission coefficient $(-)$
D	flexible mound breakwater equivalent diameter (m)
d	deep water depth (m)
E	tube Young's modulus of elasticity $(\mathrm{N\,cm^{-2}})$
f	functional symbol $(-)$
f	wave frequency (Hz)
g	gravitational acceleration $(\mathrm{m\,s^{-2}})$
H_b	breaking wave height (m)
H_i	incident wave height (m)
H_r	reflection wave height (m)
H_t	transmission wave height (m)
h	sallow water depth (m)
L	incident wave length (m)
P	internal pressure of tube (Pa)
R	crown depth
S	beach slope $(-)$
T	wave period (s)
s	spectral density $(\mathrm{cm^2\,s})$
ε	tube wall thickness (m)
ξ	Iribarren number $\xi = S/(H_b/L)^{0.5},\ (-)$
ρ	water density $(\mathrm{kg\,m^{-3}})$
ρ_s	tube density $(\mathrm{kg\,m^{-3}})$